2016 International Symposium on Nonlinear Theory and Its Applications,
NOLTA2016, Yugawara, Japan, November 27th-30th, 2016

Chaos synchronization and nonlinear dynamics in a photonic integrated circuit with two semiconductor lasers

Shoma Ohara[1], Andreas Karsaklian Dal Bosco[1], Kazusa Ugajin[1], Atsushi Uchida[1], Takahisa Harayama[2,3] and Kazuyuki Yoshimura[2,4]

[1] Department of Information and Computer Sciences, Saitama University
255 Shimo-Okubo Sakura-ku, Saitama City, Saitama 338-8570, Japan
[2] NTT Communication Science Laboratories, NTT Corporation
3-1 Morinosato, Wakamiya, Atsugi-Shi, Kanagawa 243-0198, Japan
[3] Department of Applied Physics, Waseda University
3-4-1 Okubo, Shinjuku-ku, Tokyo 169-8555, Japan
[4] Department of Information and Electronics, Graduate school of Engineering, Tottori University
4-101 Koyama-Minami, Tottori 680-8552, Japan
Emails: s16dm002@mail.saitama-u.ac.jp, auchida@mail.saitama-u.ac.jp

Abstract—We investigate the frequency dependence of chaos synchronization in a photonic integrated circuit with mutually-coupled semiconductor lasers. We calculate the cross-correlation between the two temporal waveforms of the two laser outputs with a low-pass filter. In-phase synchronization is observed between chaotic temporal waveforms of the two lasers. On the contrary, anti-phase synchronization is observed when the lasers exhibit low-frequency fluctuations (LFF).

1. Introduction

Coupled nonlinear systems show a large variety of dynamics. Recently, chaos synchronization in semiconductor lasers with delayed optical feedback has been studied for applications in secure key distribution [1, 2]. When two semiconductor lasers are mutually coupled, the output of these lasers show chaotic temporal oscillations whose dominant frequency corresponds to the inverse of twice the coupling time delay [3]. The chaotic temporal waveforms can be synchronized to each other with the time lag of the coupling delay time. In addition, anti-synchronization of low-frequency fluctuations (LFF) has been observed [4]. Episodic synchronization also has been reported when optical frequency detuning is changed [5].

The dynamics and synchronization in mutually-coupled semiconductor lasers have been investigated intensively for long coupling lengths (> 100 mm). On the contrary, photonic integrated circuits (PICs) have been proposed recently as monolithically integrated optical systems suitable for physical random number generation [6, 7]. However, the study of chaos synchronization for short coupling lengths in mutually coupled lasers has few reports. Synchronization has been performed in a particular case of two lasers exhibiting periodic oscillations in a photonic integrated circuit [8]. Nevertheless, nonlinear dynamics and chaos synchronization in a PIC with two mutually-coupled semiconductor lasers with short coupling length (~ 10 mm) have not been reported yet. It is important to investigate chaos synchronization and nonlinear dynamics in a photonic integrated circuit with mutually-coupled semiconductor lasers.

In this study, we investigate chaos synchronization in a PIC with two mutually-coupled semiconductor lasers. We focus on the dependence of the synchronization quality on different frequency components by using a low-pass filter in the LFF regime.

2. Experimental setup

We present the configuration of our photonic integrated circuit with mutually-coupled semiconductor lasers in Fig. 1. In this PIC, two semiconductor lasers, two photodetectors, a semiconductor optical amplifier (SOA), and an external mirror are monolithically integrated. The lasers are mutually coupled via the external mirror. In addition, each laser is subjected to its own optical feedback, and the corresponding external cavity lengths are 11.0 mm for laser 1 and 10.3 mm for laser 2, respectively. The parameters of the PIC are the injection currents for the laser 1, and laser 2, whose lasing threshold currents are 12.0 mA. In addition, we can change the feedback strength of laser 2 and the coupling strength between the two lasers through the SOA injection current.

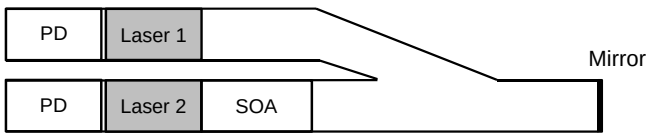

Figure 1: Schematics of photonic integrated circuit.

3. Frequency dependence of synchronization in LFF regime

The LFF dynamics consists of high-frequency chaotic oscillations and low-frequency intensity dropouts [9, 10]. We apply a low-pass filter to the laser output signals to separate these two dynamics. We calculate the cross correlation between the temporal waveforms of the laser 1 and 2 after filtering of the two laser outputs to evaluate the synchronization quality for different cut-off frequencies (1 GHz and 16 GHz) of the low-pass filter.

Figure 2 shows the temporal waveforms and the correlation plots of the output of the two lasers when the cut-off frequencies of the low-pass filter are set to 16 GHz (top) and 1 GHz (bottom), respectively. When the signals are filtered at 16 GHz, the lasers show in-phase synchronization. However, the lasers show anti-phase synchronization when the 1 GHz filter is applied. We found that the cross-correlation between the two lasers indicates a negative value for the filtered signals, while this value is positive for the unfiltered signals.

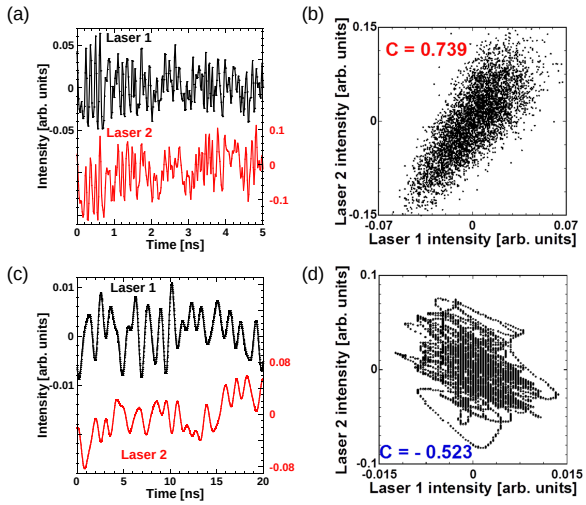

Figure 2: (a),(c) Temporal waveforms and (b),(d) correlation plots. The cut-off frequency of the low-pass filter is (a),(b) f_c = 16 GHz and (c),(d) f_c = 1 GHz. In-phase synchronization is observed at high frequency components and anti-phase synchronization is observed at low-frequency components.

Figure 3 shows the dynamics and synchronization state between both lasers when the SOA injection current (I_{SOA}) is changed. We start from a low value of I_{SOA} of 6.00 mA (Fig. 3(a)(d)), for which both laser 1 and laser 2 exhibit chaos without low-frequency predominance. When I_{SOA} is increased to 25.00 mA (Fig. 3(b)(e)), Laser 1 still exhibits chaos, while Laser 2 enters a LFF regime, as seen from the increase of low-frequency components in the RF spectrum. When I_{SOA} is further increased to 39.00 mA, both lasers exhibit LFF dynamics. Thus, changing the SOA injection current induces a change in their dynamics.

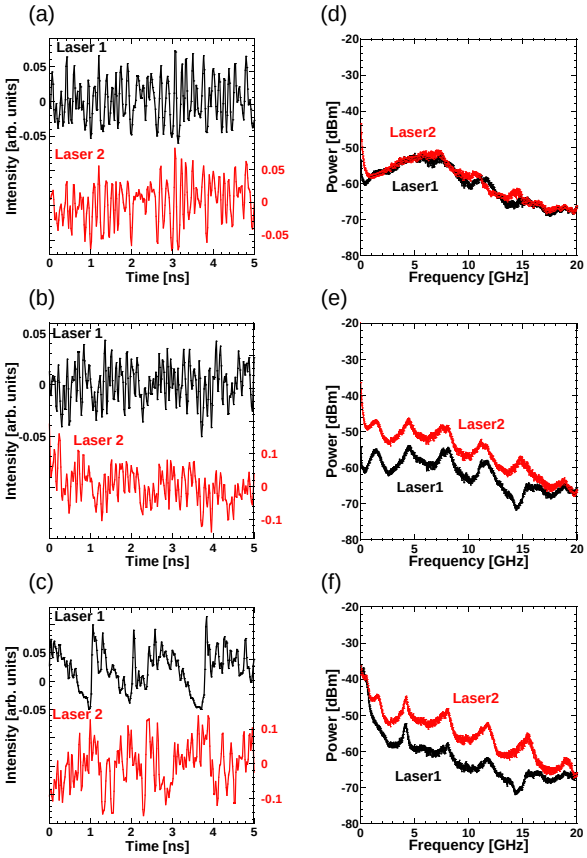

Figure 3: (a)(b)(c) Temporal waveforms and (d)(e)(f) RF spectra when the SOA injection current is changed. (a)(d) I_{SOA} = 6.00 mA, (b)(e) 25.00 mA, and (c)(f) 39.00 mA

Figure 4 shows the evolution of the peak of the cross-correlation value when the SOA injection current is changed, filtered at 1 and 16 GHz. This figure corresponds to the results of Fig. 3. We also calculate the maximum of the absolute value of the cross-correlation value for each signal because the delay time indicating the peak value changes when the cut-off frequency is changed. We discuss the dependence of the synchronization of LFF dynamics between the two lasers on the cut-off frequency of the low-pass filter. The change in the coupling strength between the two lasers results in the change in their temporal dynamics. When chaos content is dominant in both lasers (0 mA $\leqq$ I_{SOA} $\leqq$ 10 mA), in-phase oscillations are observed for both cases of 16 GHz and 1 GHz filters. When low-frequency content is dominant in both lasers (31 mA < I_{SOA} $\leqq$ 50 mA), anti-phase synchronization are obtained. When low-frequency content is dominant in one of the two lasers (21 mA $\leqq$ I_{SOA} $\leqq$ 31 mA), in-phase synchronization is observed when filtered at 16 GHz while anti-phase synchronization is obtained when filtered at 1 GHz. The synchronization state is dependent on the dynamics of each laser. Therefore, we understand that the low-frequency components of

LFF influence anti-phase synchronization.

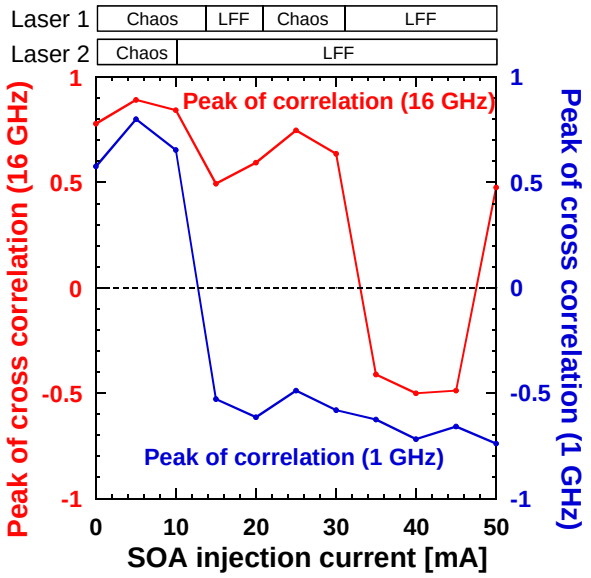

Figure 4: Cross-correlation value when the SOA injection current is changed.

4. Numerical simulations

We investigate numerical simulations with the rate equations known as the Lang-Kobayashi equations [11] in order to reproduce the experimental results as well as to give theoretical explanation. The Lang-Kobayashi equations are written as follows:

$$\frac{dE_{1,2}(t)}{dt} = \frac{1+i\alpha}{2}\left[\frac{G_N(N_{1,2}(t)-N_0)}{1+\epsilon|E_{1,2}(t)|^2}-\frac{1}{\tau_p}\right]E_{1,2}(t) + \kappa_{1,2}E_{1,2}(t-\tau_{1,2})\exp(-i\omega_{1,2}\tau_{1,2}) + \kappa_{inj}[E_{2,1}(t-\tau_{inj})\exp[i(\Delta\omega t-\omega\tau_{inj})] \quad (1)$$

$$\frac{dN_{1,2}(t)}{dt} = J_{1,2}-\frac{N_{1,2}(t)}{\tau_s}-\frac{G_N(N_{1,2}(t)-N_0)}{1+\epsilon|E_{1,2}(t)|^2}|E_{1,2}(t)|^2 \quad (2)$$

Where E and N are the complex electric field and the carrier density, respectively. $\tau_{1,2}$ and κ represent the feedback delay time and strength. τ_{inj} and κ_{inj} represent the coupling delay time and strength. α is the linewidth enhancement factor, J is the laser injection current, G_N is the gain coefficient, N_0 is the carrier density at transparency, τ_p and τ_s are the photon and carrier lifetimes. ϵ is the gain saturation coefficient. $\Delta\omega$ is the detuning of the optical angular frequencies between the two lasers. The parameter values are set as follows: $J_1 = 1.02\ J_{1,th}$, $J_2 = 1.10\ J_{2,th}$, $\kappa_1 = 0.349$, $\kappa_2 = 0.099$, $\kappa_{inj} = 0.067$, $\tau_1 = 0.29$ ns, $\tau_2 = 0.27$ ns, and $\tau_{inj} = 0.28$ ns.

We investigate the synchronization state on different frequency components by using the low-pass filter. Figure 5 shows the temporal waveforms, correlation plots, and RF spectrum for the outputs of both lasers. The cut-off frequencies are set to 16 GHz and 1 GHz in Fig. 5(a)(b) and Fig. 5(c)(d), respectively. In-phase synchronization is observed at high-frequency components, however, anti-phase synchronization is observed at low-frequency components. We focus on the RF spectrum in Fig. 5(e). The high-frequency components are dominant for laser 1, while the low frequency components are dominant for laser 2, similar to Fig. 3(b)(e). Therefore, the numerical result agrees well with the experimental result of Fig. 2 and 3.

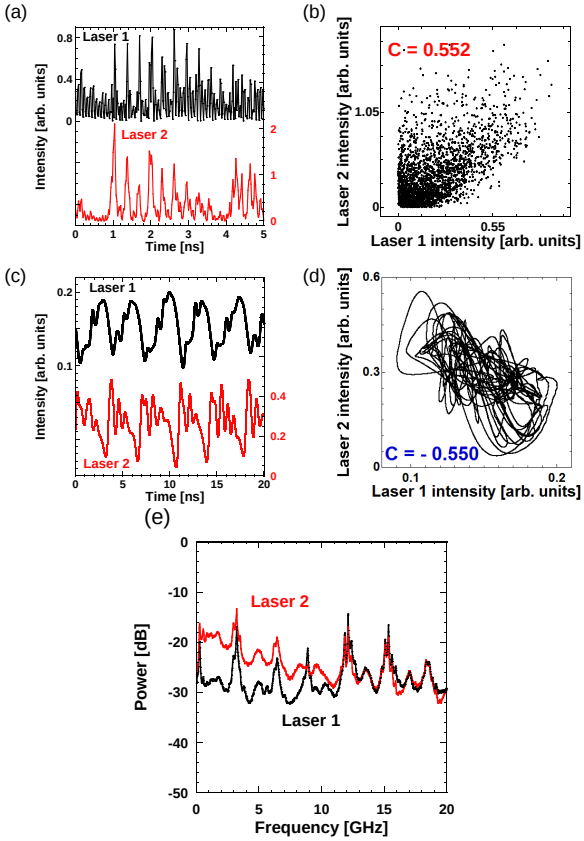

Figure 5: Numerical results of (a),(c) temporal waveforms, (b),(d) correlation plots, and (e) fast Fourier transform (FFT). The cut-off frequencies of the low-pass filter are (a)(b) 16 GHz and (c)(d) 1 GHz. In-phase synchronization is observed at high frequency components and anti-phase synchronization is observed at low-frequency components, similar to the experimental results in Fig. 2.

5. Conclusions

We investigated chaos synchronization in a photonic integrated circuit with two mutually-coupled semiconductor lasers. We applied a low pass filter with the cut-off frequency of 16 GHz or 1 GHz to the laser output signals to separate these two dynamics. We observed in-phase syn-

chronization at high-frequency components and anti-phase synchronization at low-frequency components. This result reveals the frequency dependence of chaos synchronization in the photonic integrated circuit with two mutually-coupled lasers. This phenomenon can be observed for intermediate level of the coupling strength and asymmetric optical-feedback for the two semiconductor lasers. The numerical results agree well with the experimental results.

Acknowledgments

We acknowledge support from Grants-in-Aid for Scientific Research from Japan Society for the Promotion of Science(JSPS KAKENHI Grant Number JP24686010), and Management Expenses Grants from the Ministry of Education, Culture, Sports, Science and Technology in Japan.

References

[1] K. Yoshimura, J. Muramatsu, P. Davis, T. Harayama, H. Okumura, S. Morikatsu, H. Aida, and A. Uchida, "Secure key distribution using correlated randomness in lasers driven by common random light," Physical Review Letters, Vol. 108, pp. 070602-1–5 (2012).

[2] E. Klein, N. Gross, M. Rosenbluh, W. Kinzel, L. Khaykovich, and I. Kanter, "Stable isochronal synchronization of mutually coupled chaotic lasers," Physical Review E, Vol. 73, pp. 066214-1–4 (2006).

[3] T. Heil, I. Fischer, W. Elsäßer, J. Mulet, and C. R. Mirasso, "Chaos synchronization and spontaneous symmetry-breaking in symmetrically delay-coupled semiconductor lasers," Physical Review Letters, Vol. 86, pp. 795-798 (2001).

[4] I. Wedekind and U. Parlitz, "Experimental observation of synchronization and anti-synchronization of chaotic low-frequency-fluctuations in external cavity semiconductor lasers," International Journal of Bifurcation and Chaos, Vol. 11, No. 4, 1141-1147 (2001)

[5] J. F. M. Ávila, R. Vicente, J. R. R. Leite, and C. R. Mirasso, "Synchronization properties of bidirectionally coupled semiconductor lasers under asymmetric operating conditions," Physical Review E, Vol. 75, pp. 066202-1–6 (2007).

[6] T. Harayama, S. Sunada, K. Yoshimura, P. Davis, K. Tsuzuki, and A. Uchida, "Fast nondeterministic random-bit generation using on-chip chaos lasers," Physical Review A, Vol. 83, pp. 031803-1–4(R) (2011).

[7] R. Takahashi, Y. Akizawa, A. Uchida, T. Harayama, K. Tsuzuki, S. Sunada, K. Arai, K. Yoshimura, and P. Davis, "Fast physical random bit generation with photonic integrated circuits with different external cavity lengths for chaos generation," Optics Express, Vol. 22, No. 10, pp. 11727-11740 (2014).

[8] H.-J. Wünsche, S. Bauer, J. Kreissl, O. Ushakov, N. Korneyev, F. Henneberger, E. Wille, H. Erzgrśber, M. Peil, W. Elsäßer, "Synchronization of delay-coupled oscillators: A study of semiconductor lasers," Physical Review Letters, Vol. 94, pp. 163901-1–4 (2005).

[9] T. Sano, "Antimode dynamics and chaotic itinerancy in the coherence collapse of semiconductor lasers with optical feedback," Physical Review A, Vol. 50, pp. 2719-2726 (1994).

[10] D. Brunner, M. C. Soriano, X. Porte, and I. Fischer, "Experimental phase-space tomography of semiconductor laser dynamics," Physical Review Letters, Vol. 115, pp. 053901-1–5 (2015).

[11] R. Lang and K. Kobayashi, "External optical feedback effects on semiconductor injection laser properties," IEEE Journal of Quantum Electronics, Vol. 16, No. 3, pp. 347-355 (1980).